Simulating Burr Type VII Distributions through the Method of L-moments and L-correlations

Mohan D. Pant[1] and Todd C. Headrick[2]

Abstract

Burr Type VII, a one-parameter non-normal distribution, is among the less studied distributions, especially, in the contexts of statistical modeling and simulation studies. The main purpose of this study is to introduce a methodology for simulating univariate and multivariate Burr Type VII distributions through the method of L-moments and L-correlations. The methodology can be applied in statistical modeling of events in a variety of applied mathematical contexts and Monte Carlo simulation studies. Numerical examples are provided to demonstrate that L-moment-based Burr Type VII distributions are superior to their conventional moment-based analogs in terms of distribution fitting and estimation. Simulation results presented in this study also demonstrate that the estimates of L-skew, L-kurtosis, and L-correlation are substantially superior to their conventional product-moment based counterparts of skew, kurtosis, and Pearson correlation in

[1]University of Texas at Arlington, Arlington, TX 76019, USA.
  E-mail: mpant@uta.edu
[2]Southern Illinois University Carbondale, Carbondale, IL 62901, USA.
  E-mail: headrick@siu.edu

terms of relative bias and relative efficiency when distributions with greater departure from normality are used.

1   Introduction

Of the twelve distributions introduced by Burr [1], Type VII is among the less-studied distributions. The cumulative distribution function (cdf) associated with Burr Type VII distributions is given as [1]:

$$F(x) = 2^{-k}(1 + \tanh(x))^k \tag{1}$$

where $x \in (-\infty, \infty)$ and $k > 0$ is the shape parameter, which can also be used to determine the mean and standard deviation of a distribution. The values of mean, standard deviation, skew, and kurtosis used to characterize Burr Type VII distribution—through the method of conventional moments—can be determined using the system of equations (A.4)—(A.7) as derived in the Appendix.

The Burr Type VII distributions have not received as much attention as some other Burr family of distributions (e.g., Burr Type III and Type XII distributions), especially in the context of statistical modeling and Monte Carlo simulation studies, even though they include non-normal distributions (e.g., the logistic distribution when $k = 1$) with varying degrees of skew and kurtosis. In the context of Bayesian analysis, however, Burr Type VII distributions have received some attention (e.g., see [2]). The other more widely used Burr Type III and Type XII distributions have been applied in the context of statistical modeling of events in a variety of applied mathematical contexts such as operational risk [3], forestry [4, 5], life testing [6, 7], fracture roughness [8, 9], meteorology [10],

option market price distributions [11], software reliability growth [12], reliability growth [13], and also in the context of Monte Carlo simulation studies [14, 15].

The quantile function associated with Burr Type VII distributions in (1) can be expressed as

$$q(u) = F^{-1}(x) = -\tanh^{-1}\left(1 - 2u^{1/k}\right),\qquad(2)$$

where $u \sim iid \; U(0,1)$ with pdf and cdf as 1 and u, respectively. The shape of a Burr Type VII distribution associated with (2) depends on the value of the shape parameter (k), which can be determined by solving (A.7) from the Appendix for a specified value of kurtosis (γ_4). The solved value of k can be used in (A.4)—(A.6) from the Appendix to determine the values of mean (μ), standard deviation (σ), and skew (γ_3).

In order for (2) to produce a valid Burr Type VII distribution, the quantile function $q(u)$ is required to be strictly increasing monotone function of u [14]. This requirement implies that an inverse function (q^{-1}) exists. As such, the cdf associated with (2) can be expressed as $F\left(q(u)\right) = F(u) = u$ and subsequently differentiating this cdf with respect to u will yield the parametric form of the probability density function (pdf) for $q(u)$ as $f\left(q(u)\right) = 1/q'(u)$. However, the simple closed-form expression for the pdf associated with (1) can be given as

$$f(x) = 2^{-k}k \, \text{sech}^2(x)\left(1 + \tanh(x)\right)^{k-1}\qquad(3)$$

Some of the problems associated with conventional moment-based estimates are that they can be substantially (a) biased, (b) dispersed, or (c) influenced by outliers [16, 17], and thus may not be true representatives of the parameters. To demonstrate, Figure 1 gives the graphs of the pdf and cdf associated with Burr Type VII distribution with skew $(\gamma_3) = -1.101$ and kurtosis $(\gamma_4) = 3$. These values of γ_3 and γ_4 have been obtained from Figure 2 (a), a graph of the region for feasible combinations of γ_3 and γ_4 in (A.6) and

(A.7) of the Appendix. Feasible combinations of γ_3 and γ_4 for the Burr Type VII distributions will lie on the curve graphed in Figure 2 (a). Table 1 gives the parameters and sample estimates of skew and kurtosis for the distribution in Figure 1. Inspection of Table 1 indicates that the bootstrap estimates (g_3 and g_4) of skew and kurtosis (γ_3 and γ_4) are substantially attenuated below their corresponding parameter values with greater bias and variance as the order of the estimate increases. Specifically, for sample size of $n = 50$, the values of the estimates are only 79.82%, and 53.63% of their corresponding parameters, respectively. The estimates (g_3 and g_4) of skew and kurtosis (γ_3 and γ_4) in Table 1 were calculated based on Fisher's k-statistics formulae (see, e.g., [18, pp. 299-300]), currently used by most commercial software packages such as SAS, SPSS, Minitab, etc., for computing the values of skew and kurtosis (for the standard normal distribution, $\gamma_{3,4} = 0$).

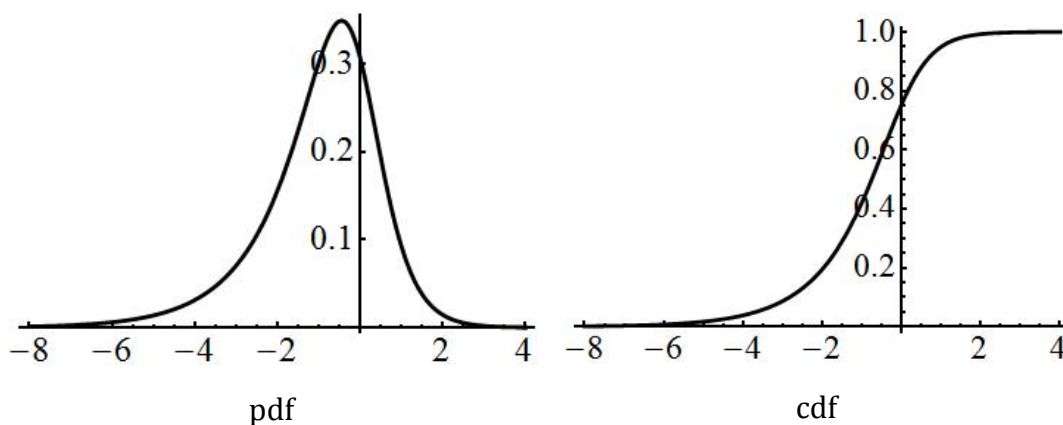Figure 1: The pdf and cdf of the Burr Type VII distribution with skew $(\gamma_3) = -1.101$ and kurtosis $(\gamma_4) = 3$. The solved value of k used in (2) and (3) is: $k = 0.406746$, which is also associated with the parameters in Tables 1 and 2.
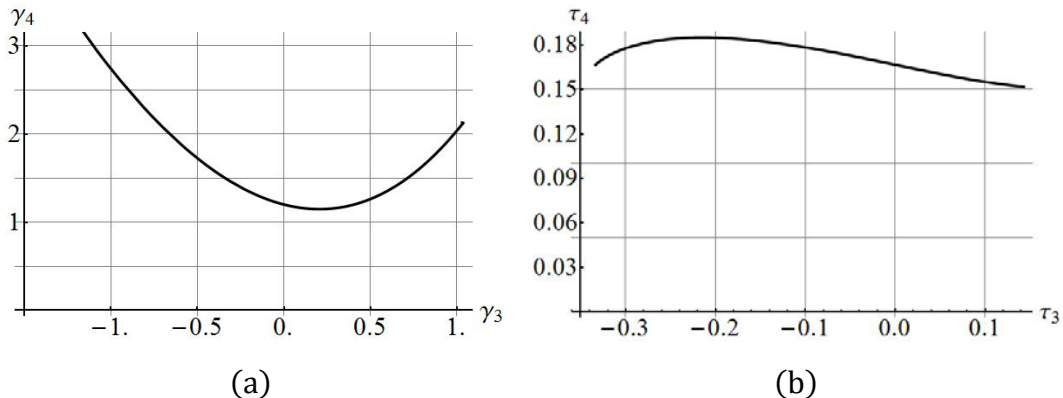
(a)   (b)

Figure 2: Graphs of the regions for possible combinations of (a) conventional moment-based skew (γ_3) and kurtosis (γ_4) and (b) L-moment-based L-skew (τ_3) and L-kurtosis (τ_4). A valid Burr Type VII distribution will lie on the curves graphed in the two panels.

Table 1: Parameter values of skew (γ_3) and kurtosis (γ_4) and their respective estimates (g_3 and g_4) for the pdf in Figure 1. Each bootstrapped estimate (Estimate), associated 95% bootstrap confidence interval (95% Bootstrap C.I.), and the standard error (St. Error) were based on resampling 25,000 statistics. Each statistic was based on a sample size of $n = 50$.

Parameter	Estimate	95% Bootstrap C.I.	St. Error
$\gamma_3 = -1.101$	$g_3 = -0.8788$	$(-0.8865, -0.8717)$	0.0038
$\gamma_4 = 3$	$g_4 = 1.609$	$(1.5808, 1.6378)$	0.0147

The method of L-moments introduced by Hosking [17] is an attractive alternative to conventional moments and can be used for describing theoretical probability distributions, fitting distributions to real-world data, estimating parameters, and testing of hypotheses [16-17, 19-20]. In these contexts, we note that the L-moment based estimators of L-skew, L-kurtosis, and L-correlation

have been introduced to address the limitations associated with conventional moment-based estimators [16-17, 19-24, 25-26]. Some qualities of L-moments that make them superior to conventional moments are that they (a) exist for any distribution with finite mean, and their estimates are (b) nearly unbiased for any sample size and less affected from sampling variability, and (c) more robust in the presence of outliers in the sample data [16-17, 19-20]. For example, the bootstrap estimates (t_3 and t_4) of L-skew and L-kurtosis (τ_3 and τ_4) in Table 2 are relatively closer to their respective parameter values with much smaller variance compared to their conventional moment-based counterparts in Table 1. Inspection of Table 2 shows that for the sample size of $n = 50$, the values of the estimates are on average 97.67% and 99.40% of their corresponding parameters.

In view of the above, the main purpose of this study is to characterize the Burr Type VII distributions through the method of L-moments in order to obviate the problems associated with conventional moment-based estimators. Another purpose of this study is to develop an L-correlation based methodology to simulate correlated Burr Type VII distributions. Specifically, in Section 2, a brief introduction to univariate L-moments is provided. The L-moment-based system of equations associated with the Burr Type VII distributions is subsequently derived. In Section 3, a comparison between conventional moment- and L-moment-based Burr Type VII distributions is presented in the contexts of distribution fitting and estimation. Numerical examples based on Monte Carlo simulation are also provided to confirm the methodology and demonstrate the advantages that L-moments have over conventional moments. In Section 4, an introduction to the coefficient of L-correlation is provided and the methodology for solving for intermediate correlations for specified L-correlation structure is subsequently presented. In Section 5, the steps for implementing the proposed L-correlation based methodology are described for simulating non-normal Burr Type VII distributions with controlled skew (L-skew), kurtosis (L-kurtosis), and Pearson correlations (L-correlations). Numerical examples and the results of

simulation are also provided to confirm the derivations and compare the new procedure with the conventional moment-based procedure. In Section 6, the results of the simulation are discussed.

Table 2: Parameter values of L-skew (τ_3) and L-kurtosis (τ_4) and their estimates $(t_3 \text{ and } t_4)$ for the pdf in Figure 1. Each bootstrapped estimate (Estimate), associated 95% bootstrap confidence interval (95% Bootstrap C.I.), and the standard error (St. Error) were based on resampling 25,000 statistics. Each statistic was based on a sample size of $n = 50$.

Parameter	Estimate	95% Bootstrap C.I.	St. Error
$\tau_3 = -0.1503$	$t_3 = -0.1468$	$(-0.1478, -0.1458)$	0.0005
$\tau_4 = 0.1827$	$t_4 = 0.1816$	$(0.1809, 0.1823)$	0.0004

2   Methodology

2.1   Theoretical and Empirical Definitions of *L*-Moments

L-moments can be expressed as certain linear combinations of probability weighted moments (PWM s). Let $X_1, \dots, X_i, \dots, X_n$ be identically and independently distributed random variables each with pdf $f(x)$, cdf $F(x)$, and the quantile function $q(u) = F^{-1}(x)$, then the PWMs are defined as in Hosking [17]

$$\beta_r = \int F^{-1}(x)\{F(x)\}^r f(x)dx \tag{4}$$

where $r = 0, 1, 2, 3$. The first four L-moments $\left(\lambda_{i=1,\dots,4}\right)$ associated with X can be expressed in simplified forms as in Hosking and Wallis [20, pp. 20-22]

$$\lambda_1 = \beta_0, \tag{5}$$

$$\lambda_2 = 2\beta_1 - \beta_0, \tag{6}$$

$$\lambda_3 = 6\beta_2 - 6\beta_1 + \beta_0, \tag{7}$$

$$\lambda_4 = 20\beta_3 - 30\beta_2 + 12\beta_1 - \beta_0, \tag{8}$$

where the coefficients associated with $\beta_{r=0,\dots,3}$ in (5)—(8) are obtained from shifted orthogonal Legendre polynomials and are computed as in [20, pp. 20-22].

The notations λ_1 and λ_2 denote the location and scale parameters. Specifically, in the literature of L-moments, λ_1 is referred to as the L-location parameter, which is equal to the arithmetic mean, and λ_2 (> 0) is referred to as the L-scale parameter and is one-half of Gini's coefficient of mean difference [18, pp. 47-48]. Dimensionless L-moment ratios are defined as the ratios of higher-order L-moments (i.e., λ_3 and λ_4) to λ_2. Thus, $\tau_3 = \lambda_3/\lambda_2$ and $\tau_4 = \lambda_4/\lambda_2$ are, respectively, the indices of L-skew and L-kurtosis. In general, the indices of L-skew and L-kurtosis are bounded in the interval $-1 < \tau_{3,4} < 1$, and as in conventional moment theory, a symmetric distribution has L-skew equal to zero [16]. The boundary region for L-skew (τ_3) and L-kurtosis (τ_4) for a continuous distribution is given by the inequality [27]

$$\frac{5\tau_3^2 - 1}{4} < \tau_4 < 1 \tag{9}$$

Empirical L-moments for a sample (of size n) of real-world data are expressed as linear combinations of the unbiased estimators of the PWMs based on sample order statistics $X_{1:n} \leq X_{2:n} \leq \cdots \leq X_{n:n}$. Specifically, the unbiased

estimators of the PWMs are given as [17, pp. 113-114]

$$b_r = \frac{1}{n} \sum_{i=r+1}^{n} \frac{(i-1)(i-2)\dots(i-r)}{(n-1)(n-2)\dots(n-r)} X_{i:n} \tag{10}$$

where $r = 0, 1, 2, 3$ and b_0 is the sample mean. The first four sample L-moments $(\ell_1, \ell_2, \ell_3, \ell_4)$ are obtained by substituting b_r from (10) instead of β_r from (4) into (5)—(8). The sample L-moment ratios (i.e., L-skew and L-kurtosis) are denoted by t_3 and t_4, where $t_3 = \ell_3/\ell_2$ and $t_4 = \ell_4/\ell_2$.

2.2 *L*-Moments for the Burr Type VII Distributions

Substituting $F^{-1}(x) = -\tanh^{-1}(1 - 2u^{1/k})$ from (2), $F(x) = u$, and $f(x) = 1$ into (4), the r-th PWM for the Burr Type VII distributions is given by

$$\beta_r = \int_0^1 -\tanh^{-1}(1 - 2u^{1/k})\, u^r\, du. \tag{11}$$

Integrating (11) for $\beta_{r=0,1,2,3}$ and substituting these PWMs into (5)—(8) and simplifying gives the following system of equations for the Burr Type VII distributions:

$$\lambda_1 = (\text{EulerGamma} + \text{PolyGamma}[0, k])/2 \tag{12}$$

$$\lambda_2 = (\text{PolyGamma}[0, 2k] - \text{PolyGamma}[0, k])/2 \tag{13}$$

$$\tau_3 = \frac{(2\text{PolyGamma}[0,3k] - 3\text{PolyGamma}[0,2k] + \text{PolyGamma}[0,k])}{(\text{PolyGamma}[0,2k] - \text{PolyGamma}[0,k])} \quad (14)$$

$$\tau_4 = (5\text{PolyGamma}[0,4k] - 10\text{PolyGamma}[0,3k] \quad\quad (15)$$
$$+ 6\text{PolyGamma}[0,2k] - \text{PolyGamma}[0,k])$$
$$/(\text{PolyGamma}[0,2k] - \text{PolyGamma}[0,k])$$

where EulerGamma $\approx .577216$ is Euler's constant and PolyGamma$[0, ik]$ for $i = 1, \dots, 4$ and $k > 0$, is a digamma function $\psi(ik)$ [28-29].

For a specified value of L-kurtosis (τ_4), (15) can be solved for positive value of k. The solved value of k can be substituted into (2) and (3) for generating the Burr Type VII distribution and its pdf, respectively. Further, the solved value of k can be substituted into (12)—(14) for computing the values of L-mean (λ_1), L-scale (λ_2), and L-skew (τ_3) associated with the Burr Type VII distribution. Provided in Figure 2 (b) is a graph of the region for feasible combinations of τ_3 and τ_4 in (14) and (15). Feasible combinations of τ_3 and τ_4 for the Burr Type VII distributions lie on the curve graphed in Figure 2 (b). In the next section, two examples are provided to demonstrate the aforementioned methodology and the advantages that L-moments have over conventional moments in the contexts of distribution fitting and estimation.

3   Advantages of L-Moments over Conventional Moments

3.1   Distribution Fitting

An example to demonstrate the advantages of L-moment-based estimation over conventional moment-based estimation is provided in Figure 3 and Table 3. Given in Figure 3 are the pdfs of the t-distribution with 8 degrees of freedom $(t_{df=8})$ superimposed, respectively, by the Burr Type VII pdfs (dashed curves) in

both (a) conventional moment- and (b) L-moment-based systems. The value of conventional moment-based shape parameter (k), given in Table 3, was determined by solving equation (A.7) from the Appendix, where the computed value of kurtosis (γ_4) associated with $t_{df=8}$ was used on the left-hand-side of (A.7). The parameter values of mean (μ), standard deviation (σ), and skew (γ_3) associated with the conventional moment-based Burr Type VII distribution, given in Table 3, were determined by substituting solved value of k into (A.4)—(A.6) from the Appendix. The solved value of k was also used in (3) to superimpose the conventional moment-based Burr Type VII pdf as shown in Figure 3 (a).

(a)   (b)
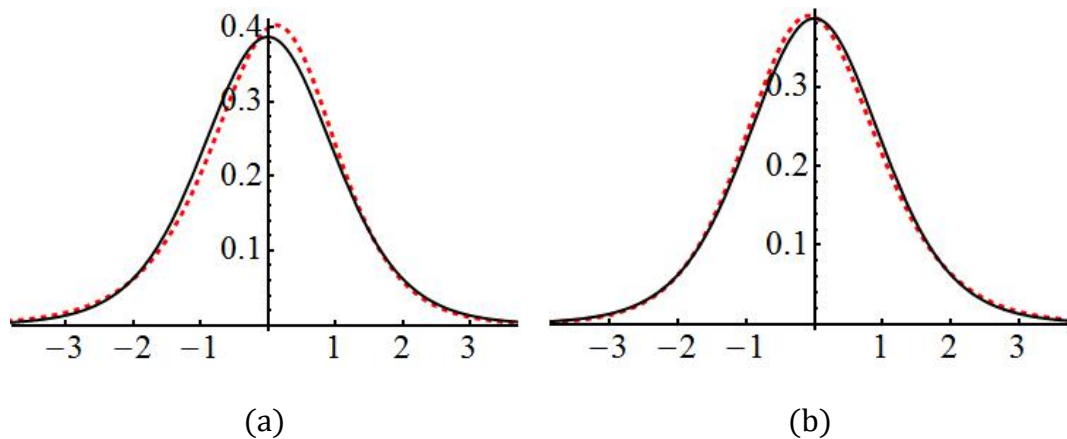
Figure 3: A pdf of t-distribution with 8 degrees of freedom $\left(t_{df=8}\right)$ superimposed by the (a) conventional moment- and (b) L-moment-based Burr Type VII pdfs (dashed curves).

The value of L-moment-based shape parameter (k), given in Table 3, was determined by solving (15), where the computed value of L-kurtosis (τ_4) associated with $t_{df=8}$ was used on the left-hand-side of (15). The parameter values of L-location (λ_1), L-scale (λ_2), and L-skew (τ_3) associated with the L-moment-based Burr Type VII distribution, given in Table 3, were determined by

substituting solved value of k into (12)—(14). The solved value of k was also substituted into (3) to superimpose the L-moment-based Burr Type VII pdf as shown in Figure 3 (b).

Table 3: Conventional moment-based parameters $(\mu, \sigma, \gamma_3, \gamma_4)$, L-moment-based parameters $(\lambda_1, \lambda_2, \tau_3, \tau_4)$, and percentiles for the t-distribution with 8 degrees of freedom $(t_{df=8})$ and the Burr Type VII approximations in Figure 3.

| Conventional moment-based parameters | L-moment-based Parameters | % | Percentiles | | |
			$t_{df=8}$ (Exact)	Conventional moment-based Burr Type VII	L-moment-based Burr Type VII
$\mu = -0.2556$	$\lambda_1 = 0.1596$	5	-1.8595	-1.9569	-1.8174
$\sigma = 1.0237$	$\lambda_2 = 0.4681$	25	-0.7064	-0.6591	-0.7215
$\gamma_3 = -0.34$	$\tau_3 = 0.0277$	50	0.0	0.0511	-0.0314
$\gamma_4 = 1.5$	$\tau_4 = 0.1632$	75	0.7064	0.7162	0.6862
$k = 0.749$	$k = 1.2248$	95	1.8595	1.781	1.925

To superimpose the Burr Type VII distribution the quantile function $q(u)$ in (2) was transformed as (a) $\left(\bar{X}\sigma - \mu S + Sq(u)\right)/\sigma$, and (b) $(\ell_1\lambda_2 - \lambda_1\ell_2 + \ell_2 q(u))/\lambda_2$, respectively, where $(\bar{X}, S)$ and (μ, σ) are the values of (mean, standard deviation), whereas (ℓ_1, ℓ_2) and (λ_1, λ_2) are the values of (L-mean, L-scale) obtained from the original $t_{df=8}$ distribution and the respective Burr Type VII approximation, respectively.

Inspection of the two panels in Figure 3 and the values of percentiles given in Table 3 illustrate that the L-moment-based Burr Type VII pdf provides a better fit to the theoretical $t_{df=8}$ distribution. The values of percentiles, given in Table 3, computed from L-moment-based Burr Type VII approximation are much closer to the exact percentiles—computed from $t_{df=8}$ distribution—than those

computed from conventional moment-based Burr Type VII approximation.

3.2   Estimation

To demonstrate the advantages of L-moment-based estimation over conventional moment-based estimation, an example is provided in Tables 6 and 7, where Monte Carlo results associated with the four Burr Type VII distributions in Figure 4 are provided. Specifically, Figure 4 provides the pdfs of the four Burr Type VII distributions, which are also used in simulating correlated Burr Type VII distributions in Section 6. Provided in Table 4 (5) are the values of conventional moment-based (L-moment-based) parameters and shape parameters of the four distributions in Figure 4.

The advantages of L-moment-based estimators over conventional moment-based estimators can also be demonstrated in the context of Burr Type VII distributions by considering the Monte Carlo simulation results associated with the indices for the percentage of relative bias (RB%) and standard error (St. Error) reported in Tables 6 and 7.

Specifically, a Fortran [30] algorithm was written to simulate 25,000 independent samples of sizes $n = 20$ and $n = 500$, and the conventional moment-based estimates (g_3 and g_4) of skew and kurtosis (γ_3 and γ_4) and the L-moment-based estimates (t_3 and t_4) of L-skew and L-kurtosis (τ_3 and τ_4) were computed for each of the $(2 \times 25{,}000)$ samples based on the parameters and the solved values of k listed in Tables 4 and 5. The estimates (g_3 and g_4) of γ_3 and γ_4 were computed based on Fisher's k-statistics formulae [18, pp. 47-48], whereas the estimates (t_3 and t_4) of τ_3 and τ_4 were computed using (5)—(8) and (10). Bias-corrected accelerated bootstrapped average estimates (Estimate), associated 95% confidence intervals (95% Bootstrap C.I.), and standard errors (St. Error) were obtained for each type of estimates using 10,000 resamples via the

commercial software package Spotfire S+ [31]. Further, if a parameter was outside its associated 95% bootstrap C.I., then the percentage of relative bias (RB%) was computed for the estimate as

$$RB\% = 100 \times (\text{Estimate} - \text{Parameter})/\text{Parameter} \qquad (16)$$

Distribution 1   Distribution 2

Distribution 3   Distribution 4
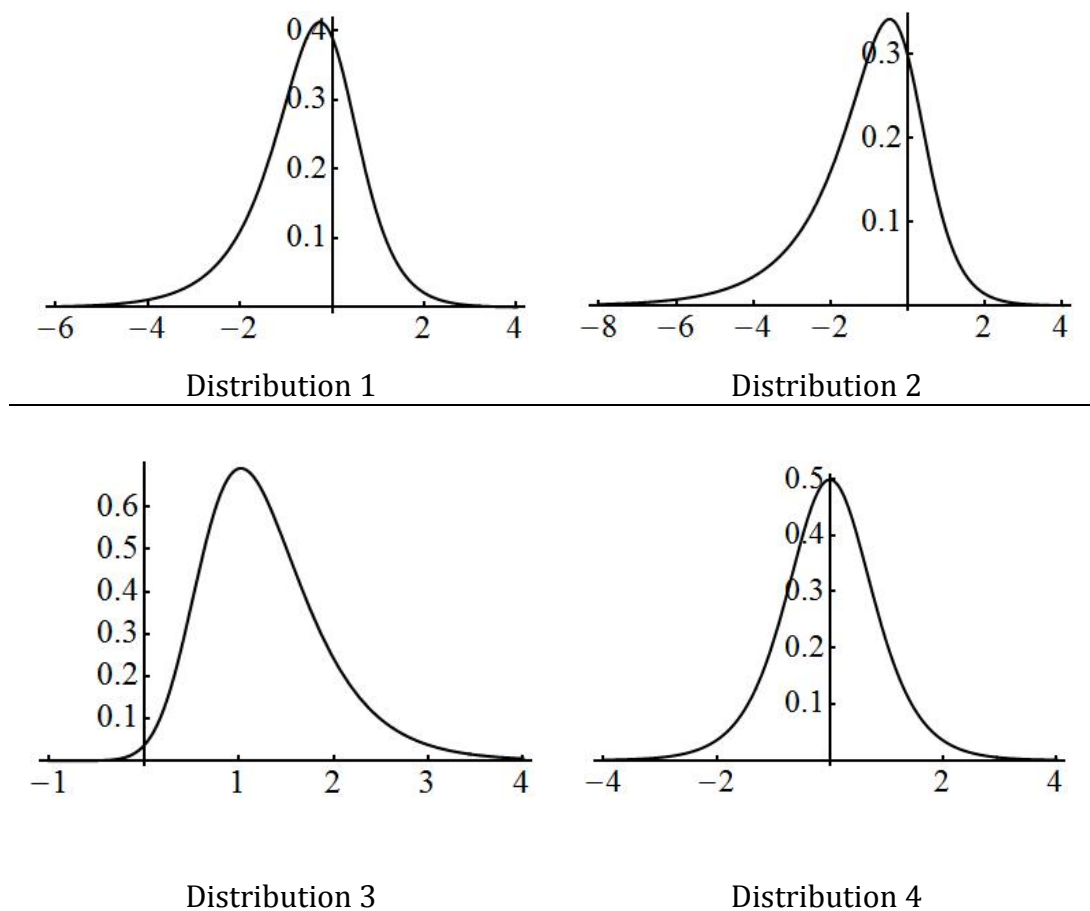
Figure 4: The pdfs of the four Burr Type VII distributions used in Monte Carlo results shown in Table 6 (7) for estimation of skew (L-skew) and kurtosis (L-kurtosis) and in Table 13 (14) for estimation of Pearson correlation (L-correlation).

Table 4: Conventional moment-based parameters of the mean (μ), standard deviation (σ), skew (γ_3), and kurtosis (γ_4) along with their corresponding values of shape parameter (k) for the four distributions in Figure 4.

Dist.	μ	σ	γ_3	γ_4	k
1	-0.5127	1.1677	-0.659	1.999	0.583363
2	-1.0335	1.5242	-1.151	3.134	0.388905
3	1.2767	0.6677	1.001	2.044	7.709897
4	-0.0059	0.9093	-0.0078	1.204	0.992841

Table 5: L-moment-based parameters of L-mean (λ_1), L-scale (λ_2), L-skew (τ_3), and L-kurtosis (τ_4) along with their corresponding values of shape parameter (k) for the four distributions in Figure 4.

Dist.	λ_1	λ_2	τ_3	τ_4	k
1	-0.5127	0.6352	-0.0876	0.1771	0.583363
2	-1.0335	0.8135	-0.1578	0.1832	0.388905
3	1.2767	0.3633	0.1463	0.1515	7.709897
4	-0.0059	0.5013	-0.0010	0.1668	0.992841

Table 6. Skew (γ_3) and Kurtosis (γ_4) results for the conventional moment-based procedure for the four distributions in Figure 4.

Dist.	Parameter	Estimate	95% Bootstrap C.I.	St. Error	RB%
			$n = 20$		
1	$\gamma_3 = -0.6590$	$g_3 = -0.3984$	$-0.4068, -0.3900$	0.00430	-39.54
	$\gamma_4 = 1.999$	$g_4 = 0.435$	$0.4177, 0.4536$	0.00917	-78.24
2	$\gamma_3 = -1.151$	$g_3 = -0.7015$	$-0.7101, -0.6935$	0.00421	-39.05
	$\gamma_4 = 3.134$	$g_4 = 0.6763$	$0.6563, 0.6982$	0.01059	-78.42
3	$\gamma_3 = 1.0014$	$g_3 = 0.6472$	$0.6398, 0.6542$	0.00368	-35.37
	$\gamma_4 = 2.044$	$g_4 = 0.3323$	$0.3147, 0.3521$	0.00951	-83.74
4	$\gamma_3 = -0.0078$	$g_3 = -0.0070$	$-0.0145, 0.0017$	0.00413	-----
	$\gamma_4 = 1.204$	$g_4 = 0.2000$	$0.1848, 0.2142$	0.00756	-83.39
			$n = 500$		
1	$\gamma_3 = -0.6590$	$g_3 = -0.6415$	$-0.6444, -0.6382$	0.00156	-2.66
	$\gamma_4 = 1.999$	$g_4 = 1.863$	$1.8484, 1.8780$	0.00756	-6.80
2	$\gamma_3 = -1.151$	$g_3 = -1.118$	$-1.1210, -1.1141$	0.00174	-2.87
	$\gamma_4 = 3.134$	$g_4 = 2.886$	$2.8646, 2.9102$	0.01143	-7.91
3	$\gamma_3 = 1.0014$	$g_3 = 0.979$	$0.9762, 0.9817$	0.00140	-2.24
	$\gamma_4 = 2.044$	$g_4 = 1.898$	$1.8803, 1.9144$	0.00869	-7.14
4	$\gamma_3 = -0.0078$	$g_3 = -0.0065$	$-0.0092, -0.0040$	0.00134	-----
	$\gamma_4 = 1.204$	$g_4 = 1.140$	$1.1318, 1.1492$	0.00443	-5.32

Table 7. L-skew (τ_3) and L-kurtosis (τ_4) results for the L-moment-based procedure for the four distributions in Figure 4.

Dist.	Parameter	Estimate	95% Bootstrap C.I.	St. Error	RB%
			$n = 20$		
1	$\tau_3 = -0.0876$	$t_3 = -0.0815$	$-0.0830, -0.0798$	0.00080	-6.96
	$\tau_4 = 0.1771$	$t_4 = 0.1742$	$0.1731, 0.1754$	0.00059	-1.64
2	$\tau_3 = -0.1578$	$t_3 = -0.1576$	$-0.1579, -0.1573$	0.00015	-----
	$\tau_4 = 0.1832$	$t_4 = 0.1831$	$0.1829, 0.1833$	0.00011	-----
3	$\tau_3 = 0.1463$	$t_3 = 0.1370$	$0.1356, 0.1385$	0.00073	-6.36
	$\tau_4 = 0.1515$	$t_4 = 0.1492$	$0.1479, 0.1502$	0.00059	-1.52
4	$\tau_3 = -0.001$	$t_3 = 0.0006$	$-0.0012, 0.0020$	0.00079	-----
	$\tau_4 = 0.1668$	$t_4 = 0.1647$	$0.1636, 0.1659$	0.00058	-1.26
			$n = 500$		
1	$\tau_3 = -0.0876$	$t_3 = -0.0874$	$-0.0877, -0.0871$	0.00016	-----
	$\tau_4 = 0.1771$	$t_4 = 0.1771$	$0.1769, 0.1773$	0.00011	-----
2	$\tau_3 = -0.1578$	$t_3 = -0.1575$	$-0.1578, -0.1572$	0.00016	-----
	$\tau_4 = 0.1832$	$t_4 = 0.1831$	$0.1829, 0.1833$	0.00011	-----
3	$\tau_3 = 0.1463$	$t_3 = 0.1460$	$0.1458, 0.1463$	0.00014	-----
	$\tau_4 = 0.1515$	$t_4 = 0.1513$	$0.1511, 0.1515$	0.00010	-----
4	$\tau_3 = -0.001$	$t_3 = -0.0011$	$-0.0014, -0.0008$	0.00015	-----
	$\tau_4 = 0.1668$	$t_4 = 0.1668$	$0.1666, 0.1670$	0.00010	-----

The results in Tables 6 and 7 illustrate that the L-moment-based estimators are superior to their conventional moment-based counterparts in terms of both smaller relative bias and error. These advantages are most pronounced in the context of smaller sample sizes and higher-order moments. For example for the Distribution 2, given a sample of size $n = 20$, the conventional moment-based estimates (g_3 and g_4) generated in the simulation were, on average, 60.95% and 21.58% of their corresponding parameters (γ_3 and γ_4). On the other hand, for the same Distribution 2, the L-moment-based estimates (t_3 and t_4) generated in the simulation study were, on average, 99.87% and 99.95% of their corresponding parameters (τ_3 and τ_4). It was also noted, for Distribution 2, that the 95% bootstrap C.I.s associated with L-moment-based estimates contained their corresponding parameters, whereas this was not the case with conventional moment-based estimates.   Thus, the relative biases of estimators based on L-moments are essentially negligible compared to those associated with the estimators based on conventional moments. Also, it can be verified that the standard errors associated with the estimates t_3 and t_4 are relatively much smaller and more stable than the standard errors associated with the estimates g_3 and g_4.

4   *L*-Correlations for the Burr Type VII Distributions

Let Y_j and Y_k be two random variables with cdfs $F(Y_j)$ and $F(Y_k)$ respectively. The second L-moments of Y_j and Y_k can be defined as in [26]

$$\lambda_2(Y_j) = 2Cov\left(Y_j, F(Y_j)\right) \tag{17}$$

$$\lambda_2(Y_k) = 2Cov\left(Y_k, F(Y_k)\right) \tag{18}$$

The second L-comoment of Y_j toward Y_k and Y_k toward Y_j are given as

$$\lambda_2(Y_j, Y_k) = 2Cov\left(Y_j, F(Y_k)\right) \tag{19}$$

$$\lambda_2(Y_k, Y_j) = 2Cov\left(Y_k, F(Y_j)\right) \tag{20}$$

The *L*-correlations of Y_j toward Y_k and Y_k toward Y_j are subsequently defined as:

$$\eta_{jk} = \frac{\lambda_2(Y_j, Y_k)}{\lambda_2(Y_j)} \tag{21}$$

$$\eta_{kj} = \frac{\lambda_2(Y_k, Y_j)}{\lambda_2(Y_k)} \tag{22}$$

The *L*-correlation given in (21) (or, 22) is bounded in the interval: $-1 \le \eta_{jk} \le 1$. A value of $\eta_{jk} = 1$ $\left(\text{or}, \eta_{jk} = -1\right)$ implies that Y_j and Y_k have a strictly and monotonically increasing (or, decreasing) relationship. See Serfling and Xiao [26] for further details on the topics related to the *L*-correlation.

The extension of the Burr Type VII distributions to multivariate level can be obtained by specifying T quantile functions as given in (2) with a specified L-correlation structure. Specifically, let $Z_1, \ldots, Z_T$ denote standard normal variables with cdfs and the joint pdf associated with Z_j and Z_k given by the following expressions:

$$\Phi(Z_j) = \int_{-\infty}^{Z_j} (2\pi)^{-1/2} \exp\left\{-v_j^2/2\right\} dv_j \tag{23}$$

$$\Phi(Z_k) = \int_{-\infty}^{Z_k} (2\pi)^{-1/2} \exp\{-v_k^2/2\} dv_k \tag{24}$$

$$f_{jk} = \left(2\pi(1 - r_{jk}^2)^{1/2}\right)^{-1} \exp\left\{-\left(2(1 - r_{jk}^2)\right)^{-1}\left(z_j^2 + z_k^2 - 2r_{jk}z_jz_k\right)\right\}. \tag{25}$$

where r_{jk} in (25) is the intermediate correlation (IC) between Z_j and Z_k. Using the cdf s in (23) and (24) as zero-one uniform deviates, i.e., $\Phi(Z_j), \Phi(Z_k) \sim U(0, 1)$, the quantile function defined in (2) can be expressed as a function of $\Phi(Z_j)$, or $\Phi(Z_k)$ $\left(\text{e.g.,} \ q_j\left(\Phi(Z_j)\right) \text{or} \ q_k(\Phi(Z_k))\right)$. Thus, the

L-correlation of $Y_j = q_j\left(\Phi(Z_j)\right)$ toward $Y_k = q_k\left(\Phi(Z_k)\right)$ can be determined using (21) with the denominator standardized to $\lambda_2(Y_j) = 1/\sqrt{\pi}$ for the standard normal distribution as

$$\eta_{jk} = 2\sqrt{\pi} \int_{-\infty}^{\infty}\int_{-\infty}^{\infty} x_j\left(q_j\left(\Phi(Z_j)\right)\right)\Phi(z_k)\,f_{jk}\,dz_j dz_k. \tag{26}$$

The variable $x_j\left(q_j\left(\Phi(Z_j)\right)\right)$ in (26) is the standardized quantile function of (2) such that it has an L-mean (or, arithmetic mean) of zero and L-scale equal to that of the standard normal distribution. That is, the quantile function $Y_j = q_j\left(\Phi(Z_j)\right)$ is standardized by a linear transformation as

$$x_j\left(q_j\left(\Phi(Z_j)\right)\right) = \delta\left(q_j\left(\Phi(Z_j)\right) - \lambda_1\right) \tag{27}$$

where λ_1 is the mean from (12) and δ is a constant that scales λ_2 in (13) and in the denominator of (21) to $1/\sqrt{\pi}$. In particular, δ for the Burr Type VII distributions can be expressed as

$$\delta = -\frac{2}{\sqrt{\pi}(\text{PolyGamma}[0,k] - \text{PolyGamma}[0,2k])} \tag{28}$$

The next step is to use (26) to solve for the values of the $T(T-1)/2$ ICs (r_{jk}) such that the T specified Burr Type VII distributions have their specified L-correlation structure.

Analogously, the L-correlation of $Y_k = q_k\left(\Phi(Z_k)\right)$ toward $Y_j = q_j\left(\Phi(Z_j)\right)$ is given as

$$\eta_{kj} = 2\sqrt{\pi} \int_{-\infty}^{\infty} \int_{-\infty}^{\infty} x_k \left(q_k(\Phi(Z_k)) \right) \Phi(z_j) \, f_{jk} \, dz_k dz_j. \tag{29}$$

Note that in general, the L-correlation of $Y_j = q_j \left(\Phi(Z_j) \right)$ toward $Y_k = q_k(\Phi(Z_k))$ in (26) is not equal to the L-correlation of $Y_k = q_k(\Phi(Z_k))$ toward $Y_j = q_j \left(\Phi(Z_j) \right)$ in (29). These L-correlations are equal only when the values of shape parameters k associated with $q_j \left(\Phi(Z_j) \right)$ and $q_k(\Phi(Z_k))$ are equal (i.e., when the two distributions are the same). Provided in Algorithm 1 is a source code written in Mathematica [28-29], which shows an example for computing ICs $\left(r_{jk} \right)$ for the L-correlation procedure. The steps for simulating correlated Burr Type VII distributions with specified values of L-skew (τ_3), L-kurtosis (τ_4), and with specified L-correlation structure are given in Section 5.

5   Steps for Monte Carlo Simulation with an Example

The procedure for simulating Burr Type VII distributions with specified L-moments and L-correlations can be summarized in the following six steps:

1. Specify the L-moments for T transformations of the form in (2), i.e., $q_1(\Phi(z_1)), \dots, q_T(\Phi(z_T))$ and obtain the solutions for the shape parameter k by solving (15) for the specified value of L-kurtosis (τ_4) for each distribution. Specify a $T \times T$ matrix of L-correlations (η_{jk}) for $q_j(\Phi(z_j))$ toward $q_k(\Phi(Z_k))$, where $j < k \in \{1, 2, \dots, T\}$.

2. Compute the values of intermediate (Pearson) correlations (ICs), r_{jk}, by substituting the value of specified L-correlation (η_{jk}) and the solved value of k from Step 1 into the left- and the right-hand sides of (26), respectively, and then numerically integrating (26) to solve for r_{jk}. See

Algorithm 1 for an example. Repeat this step separately for all $T(T-1)/2$ pairwise combinations of ICs.

3. Assemble the ICs computed in Step 2 into a $T \times T$ matrix and then decompose this matrix using Cholesky factorization. Note that this step requires the IC matrix to be positive definite.

4. Use elements of the matrix resulting from Cholesky factorization of Step 3 to generate T standard normal variables $(Z_1, \dots, Z_T)$ correlated at the IC levels as follows:

$$Z_1 = a_{11}V_1$$

$$Z_2 = a_{12}V_1 + a_{22}V_2$$

$$\vdots$$

$$Z_j = a_{1j}V_1 + a_{2j}V_2 + \cdots + a_{ij}V_i + \cdots + a_{jj}V_j \qquad (30)$$

$$\vdots$$

$$Z_T = a_{1T}V_1 + a_{2T}V_2 + \cdots + a_{iT}V_i + \cdots + a_{jT}V_T + \cdots + a_{TT}V_T$$

where $V_1, \dots, V_T$ are independent standard normal random variables and where a_{ij} is the element in the i-th row and j-th column of the matrix resulting from Cholesky factorization of Step 3.

5. Substitute $Z_1, \dots, Z_T$ from Step 4 into the following Taylor series-based expansion for computing the cdf, $\Phi(Z_j)$, of standard normal distribution [32]

$$\Phi(Z_j) = \left(\frac{1}{2}\right) + \phi(Z_j)\left\{Z_j + \frac{Z_j^3}{3} + \frac{Z_j^5}{(3 \cdot 5)} + \frac{Z_j^7}{(3 \cdot 5 \cdot 7)} + \cdots\right\} \qquad (31)$$

where $\phi(Z_j)$ is the pdf of standard normal distribution and the absolute error associated with (31) is less than 8×10^{-16}.

6. Substitute the uniform (0, 1) variables, $\Phi(Z_j)$, generated in Step 5 into the T equations of the form $q_j(\Phi(z_j))$ in (2) to generate the Burr Type VII distributions with specified values of L-skew (τ_3), L-kurtosis (τ_4), and with specified L-correlation structure.

For the purpose of evaluating the proposed methodology and demonstrating the steps above, an example is subsequently provided to compare the L-correlation-based procedure with the conventional product moment-based Pearson correlation procedure. Specifically, the distributions in Figure 4 are used as a basis for a comparison using the specified correlation matrix in Table 8 where strong correlations are considered. Let the four distributions in Figure 4 be denoted as $Y_1 = q_1(\Phi(Z_1))$, $Y_2 = q_2(\Phi(Z_2))$, $Y_3 = q_3(\Phi(Z_3))$, and $Y_4 = q4\Phi Z4$, where *Y1*, *Y2*, *Y3*, and *Y4* are the quantile functions from (2). The specified values of conventional moments and L-moments together with shape parameters (k) associated with these four distributions are given in Tables 4 and 5, respectively. Presented in Tables 9 and 10 are the intermediate correlations (ICs) obtained for the conventional product moment-based Pearson correlation and L-moment-based L-correlation procedures, respectively, for the distributions in Figure 4. Provided in Algorithm 2 is a source code written in Mathematica [28-29], which shows an example for computing ICs (r_{jk}) for the conventional product moment-based Pearson correlation procedure. See, also Headrick, Pant, and Sheng [14, pp. 2217-2221] for a detailed methodology for simulating correlated Burr Type III and Type XII distributions through the method of Pearson correlation.

Provided in Tables 11 and 12 are the results of Cholesky factorization on the IC matrices in Tables 9 and 10, respectively. The elements of matrices in Tables 11 and 12 are used to generate $Z_1, ..., Z_4$ correlated at the IC levels by making use of the formulae (30) in Step 4, above, with $T = 4$. The values of $Z_1, ..., Z_4$ are then used in (31) to obtain the Taylor series-based approximations

of the cdfs $\Phi(Z_1)$, $\Phi(Z_2)$, $\Phi(Z_3)$, and $\Phi(Z_4)$, which are treated as uniform $(0,1)$ variables. These uniform variables are used in (2) to obtain the quantile functions $q_1\big(\Phi(Z_1)\big)$, $q_2\big(\Phi(Z_2)\big)$, $q_3\big(\Phi(Z_3)\big)$, and $q_4\big(\Phi(Z_4)\big)$ to generate the four distributions in Figure 4 that are correlated at the specified correlation level of Table 8.

For the Monte Carlo simulation, a Fortran [30] algorithm was written for both procedures to generate 25,000 independent sample estimates for the specified parameters of (a) conventional product moment-based Pearson correlation (ρ_{jk}), and (b) L-moment-based L-correlation (η_{jk}) based on samples of sizes $n = 20$ and $n = 500$. The estimate for ρ_{jk} was based on the usual formula for the Pearson correlation statistic. The estimate of η_{jk} was computed by substituting (17) and (19) into (21), where the empirical forms of the cdfs were used in (17) and (19). The sample estimates ρ_{jk} and η_{jk} were both transformed using Fisher's z' transformations. Bias-corrected accelerated bootstrapped average estimates (Estimate), 95% bootstrap confidence intervals (95% Bootstrap C.I.), and standard errors (St. Error) were obtained for the estimates associated with the parameters $\left(z'_{(\rho_{jk})} \text{ and } z'_{(\eta_{jk})}\right)$ using 10,000 resamples via the commercial software package Spotfire S+ [31]. The bootstrap results associated with the estimates of $z'_{(\rho_{jk})}$ and $z'_{(\eta_{jk})}$ were transformed back to their original metrics. Further, if a parameter was outside its associated 95% bootstrap C.I., then the percentage of relative bias (RB%) was computed for the estimate as in (16). The results of this simulation are presented in Tables 13 and 14, and are discussed in Section 6.

Table 8: Specified correlation matrix for the conventional moment- and *L*-moment-based procedures for the four distributions in Figure 4.

Dist.	1	2	3	4
1	1.00			
2	0.70	1.00		
3	0.80	0.70	1.00	
4	0.85	0.75	0.75	1.00

Table 9: Intermediate correlation matrix for the conventional moment-based Pearson correlation procedure.

Dist.	1	2	3	4
1	1.0			
2	0.712802	1.0		
3	0.845154	0.763062	1.0	
4	0.858634	0.771204	0.768917	1.00

Table 10: Intermediate correlation matrix for the *L*-moment-based *L*-correlation procedure.

Dist.	1	2	3	4
1	1.0			
2	0.691496	1.0		
3	0.793033	0.690632	1.0	
4	0.844246	0.741316	0.745811	1.00

Table 11: Matrix obtained from Cholesky decomposition on the intermediate correlation matrix in Table 9.

$a_{11} = 1.00$	$a_{12} = 0.712802$	$a_{13} = 0.845154$	$a_{14} = 0.858634$
$a_{21} = 0.00$	$a_{22} = 0.701365$	$a_{23} = 0.229031$	$a_{24} = 0.226940$
$a_{31} = 0.00$	$a_{32} = 0.0$	$a_{33} = 0.482970$	$a_{34} = -0.018091$
$a_{41} = 0.00$	$a_{42} = 0.0$	$a_{43} = 0.0$	$a_{44} = 0.459258$

Table 12: Matrix obtained from Cholesky decomposition on the intermediate correlation matrix in Table 10.

$a_{11} = 1.00$	$a_{12} = 0.691496$	$a_{13} = 0.793033$	$a_{14} = 0.844246$
$a_{21} = 0.00$	$a_{22} = 0.722380$	$a_{23} = 0.196922$	$a_{24} = 0.218061$
$a_{31} = 0.00$	$a_{32} = 0.0$	$a_{33} = 0.576473$	$a_{34} = 0.057861$
$a_{41} = 0.00$	$a_{42} = 0.0$	$a_{43} = 0.0$	$a_{44} = 0.486159$

6 Discussion and Conclusion

One of the advantages of L-moment-based procedure over conventional moment-based procedure can be highlighted in the context of estimation. The L-moment-based estimators of L-skew and L-kurtosis can be far less biased than the conventional moment-based estimators of skew and kurtosis when samples are drawn from the distributions with greater departure from normality [15-16, 19-24, 26]. Inspection of the simulation results in Tables 6 and 7 clearly indicates that this is the case for the Burr Type VII distributions. That is, the superiority that estimates of L-moment ratios (τ_3 and τ_4) have over their corresponding conventional moment-based estimates of skew and kurtosis (γ_3 and γ_4) is

obvious. For example, for samples of size $n = 20$, the estimates of γ_3 and γ_4 for Distribution 2 were, on average, 60.95% and 21.58% of their corresponding parameters, whereas the estimates of τ_3 and τ_4 were 99.87% and 99.95% of their corresponding parameters. Also, for Distribution 2, the 95% bootstrap C.I.s associated with estimates of τ_3 and τ_4 contained their corresponding parameters, whereas the corresponding C.I.s associated with estimates of γ_3 and γ_4 contained none of the population parameters. Further, for large sample sizes $(n = 500)$, the 95% bootstrap C.I.s associated with estimates of τ_3 and τ_4 for all four distributions in Figure 4 contained the population parameters, whereas the corresponding C.I.s associated with estimates of γ_3 and γ_4 contained none of the population parameters. This advantage of L-moment-based estimates can also be expressed by comparing their relative standard errors (RSEs), where RSE = {(St. Error/Estimate) $\times$ 100}. Comparing Tables 6 and 7, it is evident that the estimates of τ_3 and τ_4 are more efficient as their RSEs are considerably smaller than the RSEs associated with the conventional moment-based estimates of γ_3 and γ_4. For example, in terms of Distribution 2 in Figure 4, inspection of Tables 6 and 7 (for $n = 500$), indicates that RSE measures of: RSE $(t_3) = 0.10\%$ and RSE $(t_4) = 0.06\%$ are considerably smaller than the RSE measures of: RSE $(g_3) = 0.16\%$ and RSE $(g_4) = 0.40\%$. This demonstrates that the estimates of L-skew and L-kurtosis have more precision because they have less variance around their bootstrapped estimates.

Another advantage of L-moment-based procedure over conventional moment-based procedure can be highlighted in the context of distribution fitting. In the context of distribution fitting, the L-moment-based Burr Type VII pdf in Figure 3 (b) provides a better fit to the theoretical t-distribution with 8 degrees of freedom $\left(t_{df=8}\right)$ than the conventional moment-based Burr Type VII pdf in Figure 3 (a).

Presented in Tables 13 and 14 are the simulation results of conventional product moment-based Pearson correlations and L-moment-based L-correlations,

respectively. Overall inspection of these tables indicates that the L-correlation is superior to Pearson correlation in terms of relative bias. For example, for $n = 20$, the percentage of relative bias for the two distributions, Distribution 2 and Distribution 3, in Figure 4 was   3.74% for the Pearson correlation compared with only 1.59% for the L-correlation. Further, for large sample sizes $(n = 500)$, the 95% bootstrap C.I.s associated with L-correlation estimate contained almost all of the population parameters, whereas the corresponding C.I.s associated with Pearson correlation estimate contained none of the population parameters. It is also noted that the variability associated with bootstrapped estimates of L-correlation appears to be more stable than that of the bootstrapped estimates of Pearson correlation both within and across different conditions.

In summary, the new L-moment-based procedure is an attractive alternative to the more traditional conventional moment-based procedure in the context of Burr Type VII distributions. In particular, the L-moment-based procedure has distinct advantages when distributions with greater departures from normality are used. Finally, we note that Mathematica [28-29] source codes are available from the authors for implementing both the conventional moment- and L-moment-based procedures.

Table 13: Correlation results for the conventional product moment-based Pearson correlations.

$$n = 20$$

Parameter	Estimate	95% Bootstrap C.I.	St. Error	RB%
$\rho_{12} = 0.70$	0.7151	(0.7135, 0.7166)	0.00160	2.16
$\rho_{13} = 0.80$	0.8204	(0.8195, 0.8212)	0.00133	2.55
$\rho_{14} = 0.85$	0.8596	(0.8588, 0.8603)	0.00153	1.13
$\rho_{23} = 0.70$	0.7262	(0.7250, 0.7275)	0.00131	3.74
$\rho_{24} = 0.75$	0.7662	(0.7648, 0.7672)	0.00150	2.16
$\rho_{34} = 0.75$	0.7649	(0.7635, 0.7660)	0.00150	1.99

$$n = 500$$

Parameter	Estimate	95% Bootstrap C.I.	St. Error	RB%
$\rho_{12} = 0.70$	0.7008	(0.7005, 0.7011)	0.00032	0.11
$\rho_{13} = 0.80$	0.8009	(0.8007, 0.8011)	0.00025	0.11
$\rho_{14} = 0.85$	0.8502	(0.8502, 0.8505)	0.00029	0.02
$\rho_{23} = 0.70$	0.7013	(0.7011, 0.7016)	0.00023	0.19
$\rho_{24} = 0.75$	0.7507	(0.7504, 0.7509)	0.00029	0.09
$\rho_{34} = 0.75$	0.7505	(0.7502, 0.7507)	0.00028	0.07

Table 14: Correlation results for the L-moment-based L-correlation procedure.

$$n = 20$$

Parameter	Estimate	95% Bootstrap C.I.	St. Error	RB%
$\eta_{12} = 0.70$	0.7113	(0.7096, 0.7129)	0.00168	1.60
$\eta_{13} = 0.80$	0.8093	(0.8082, 0.8105)	0.00171	1.16
$\eta_{14} = 0.85$	0.8581	(0.8571, 0.8589)	0.00170	0.95
$\eta_{23} = 0.70$	0.7111	(0.7093, 0.7127)	0.00171	1.59
$\eta_{24} = 0.75$	0.7608	(0.7595, 0.7623)	0.00168	1.44
$\eta_{34} = 0.75$	0.7616	(0.7602, 0.7630)	0.00173	1.55

$$n = 500$$

Parameter	Estimate	95% Bootstrap C.I.	St. Error	RB%
$\eta_{12} = 0.70$	0.7003	(0.6999, 0.7006)	0.00030	-----
$\eta_{13} = 0.80$	0.8001	(0.7999, 0.8004)	0.00030	-----
$\eta_{14} = 0.85$	0.8500	(0.8499, 0.8503)	0.00030	-----
$\eta_{23} = 0.70$	0.7003	(0.6999, 0.7006)	0.00031	-----
$\eta_{24} = 0.75$	0.7502	(0.7499, 0.7504)	0.00031	-----
$\eta_{34} = 0.75$	0.7503	(0.7501, 0.7506)	0.00030	0.04

(* Intermediate Correlation *)

$r_{12} = 0.691496;$

Needs["MultivariateStatistics`"]

$f_{12} = $ PDF[MultinormalDistribution[$\{0, 0\}, \{\{1, r_{12}\}, \{r_{12}, 1\}\}], \{Z_1, Z_2\}$];

$\Phi_1 = $ CDF[NormalDistribution[0, 1], Z_1];

$\Phi_2 = $ CDF[NormalDistribution[0, 1], Z_2];

(* Parameters for Distribution 1 and Distribution 2 in Figure 4 *)

$k_1 = 0.583363;$

$\lambda_1 = -0.512657;$

$\delta_1 = 0.888151;$

 (* Quantile function from (2) can alternatively be written as *)

$y_1 = -\frac{1}{2}\text{Log}\left[\Phi_1^{(-1/k_1)} - 1\right];$

(* Standardizing constants λ_1 and δ_1 were obtained, respectively, from (12) and (28) *)

$x_1 = \delta_1 * (y_1 - \lambda_1);$

(* Compute the value of specified L-correlation *)

$\eta_{12} = 2\sqrt{\pi} *$NIntegrate[$x_1 * \Phi_2 * f_{12}, \{Z_1, -8, 8\}, \{Z_2, -8, 8\}$, Method $\rightarrow$ "MultiDimensionalRule"]

0.70

Algorithm 1: Mathematica source code for computing intermediate correlations for specified L-correlations. The example is for Distribution $j = 1$ toward Distribution $k = 2$ (η_{12}). See pdfs of Distribution 1 and Distribution 2 in Figure 4, specified correlation in Table 8, and intermediate correlation in Table 10.

(* Intermediate Correlation *)

$r_{12} = 0.712802;$

Needs["MultivariateStatistics`"]

$f_{12} = \text{PDF}[\text{MultinormalDistribution}[\{0, 0\}, \{\{1, \ r_{12}\}, \{r_{12}, 1\}\}], \{Z_1, \ Z_2\}];$

$\Phi_1 = \text{CDF}[\text{NormalDistribution}[0, 1], \ Z_1];$

$\Phi_2 = \text{CDF}[\text{NormalDistribution}[0, 1], \ Z_2];$

(* Parameters for Distribution 1 and Distribution 2 in Figure 4 *)

$k_1 \ = \ 0.583363;$

$\mu_1 = -0.512657;$

$\sigma_1 = 1.167658;$

$k_2 \ = \ 0.388905;$

$\mu_2 = -1.033464;$

$\sigma_2 = 1.524227;$

(* Quantile functions from (2) can alternatively be written as *)

$$y_1 = -\frac{1}{2}\text{Log}\left[\Phi_1^{(-1/k_1)} - 1\right]$$

$$y_2 = -\frac{1}{2}\text{Log}\left[\Phi_2^{(-1/k_2)} - 1\right]$$

(* Standardizing constants μ_1, μ_2 and σ_1, σ_2 are obtained, respectively, from (A.4) and (A.5) from the Appendix *)

$x_1 = (y_1 - \mu_1)/\sigma_1;$

$x_2 = (y_2 - \mu_2)/\sigma_2;$

(* Specified conventional product moment-based Pearson correlation *)

$\rho_{12} = \ \text{NIntegrate}[\ x_1 * x_2 * f_{12}, \ \{Z_1, \ -8, \ 8\}, \ \{Z_2, \ -8, \ 8\}, \ \text{Method} \ \rightarrow$ "MultiDimensionalRule"]

0.70

Algorithm 2: Mathematica source code for computing intermediate correlations for specified conventional product moment-based Pearson correlations. The example is for Distribution $j = 1$ and Distribution $k = 2$ (ρ_{12}). See pdfs of Distribution 1 and Distribution 2 in Figure 4, specified correlation in Table 8, and intermediate correlation in Table 9.

References

[1] I. W. Burr, Cumulative frequency functions, *The Annals of mathematical statistics*, **13**(2), (1942), 215-232.

[2] N. Feroze and M. Aslam, On Bayesian analysis of Burr type VII distribution under different censoring schemes, *International Journal of Quality, Statistics and Reliability*, **vol. 2012**, Article ID 248146, 5 pages, (2012). doi:10.1155/2012/248146

[3] A. S. Chernobai, F. J. Fabozzi, and S. T. Rachev, *Operational Risk: A Guide to Basel II Capital Requirements, Models, and Analysis*, John Wiley & Sons, NY, USA, 2007.

[4] J. H. Gove, M. J. Ducey, W. B. Leak, and L. Zhang, Rotated sigmoid structures in managed uneven-aged northern hardwood stands: A look at the Burr Type III distribution, *Forestry*, **81**, (2008), 161-176.

[5] S. R. Lindsay, G. R. Wood, and R. C. Woollons, Modelling the diameter distribution of forest stands using the Burr distribution, *Journal of Applied Statistics*, **23**, (1996), 609-619.

[6] D. R. Wingo, Maximum likelihood methods for fitting the burr type XII distribution to life test data, *Biometrical Journal*, **25**, (1983), 77-84.

[7] D. R. Wingo, Maximum likelihood methods for fitting the burr type XII distribution to multiply (progressively) censored life test data, *Metrika*, **40**, (1993), 203-210.

[8] S. Nadarajah and S. Kotz, q exponential is a Burr distribution, *Physics Letters A*, **359**, (2006), 577-579.

[9] S. Nadarajah and S. Kotz, On the alternative to the Weibull function, *Engineering Fracture Mechanics*, **74**, (2007), 451-456.

[10] P. W. Mielke, Another family of distributions for describing and analyzing precipitation data, *Journal of Applied Meteorology*, **12**, (1973), 275–280.

[11] B. J. Sherrick, P. Garcia, and V. Tirupattur, Recovering probabilistic information from option markets: Tests of distributional assumptions, *Journal of Future Markets*, **16**, (1996), 545–560.

[12] A. A. Abdel-Ghaly, G. R. Al-Dayian, and F. H. Al-Kashkari, The use of Burr Type XII distributions on software reliability growth modelling, *Microelectronics Reliability*, **37**, (1997), 305-313.

[13] N. A. Mokhlis, Reliability of a stress-strength model with Burr type III distributions, *Communications in Statistics-Theory and Methods*, **34**, (2005), 1643–1657.

[14] T. C. Headrick, M. D. Pant, and Y. Sheng, On simulating univariate and multivariate Burr Type III and Type XII distributions, *Applied Mathematical Sciences*, **4**(45), (2010), 2207–2240. http://www.m-hikari.com/ams/ams-2010 /ams-45-48-2010/index.html

[15] M. D. Pant and T. C. Headrick, A method for simulating Burr Type III and Type XII distributions through *L*-moments and *L*-correlations, *ISRN Applied Mathematics*, **vol. 2013**, Article ID 191604, 14 pages, (2013). doi:10.1155/2013/191604

[16] T. C. Headrick, A characterization of power method transformations through *L*-moments, *Journal of Probability and Statistics*, **vol. 2011**, Article ID 497463, 22 pages, (2011). doi: 10.1155/2011/497463

[17] J. R. M. Hosking, L-moments: Analysis and estimation of distributions using linear combinations of order statistics, *Journal of the Royal Statistical Society*, *Series B*, **52**(1), (1990), 105–124.

[18] M. Kendall and A. Stuart, *The Advanced Theory of Statistics*, Fourth edition, Macmillan, New York, USA, 1977.

[19] J. R. M. Hosking, Moments or *L*-moments? An example comparing two measures of distributional shape, *American Statistician*, **46**(3), (1992), 186-189.

[20] J. R. M. Hosking and J. R. Wallis, *Regional frequency analysis: An approach based on L-moments*, Cambridge University Press, Cambridge, UK, 1997.

[21] T. C. Headrick and M. D. Pant, Simulating non-normal distributions with specified L-moments and L-correlations, *Statistica Neerlandica*, **66**(4), (2012), 422–441. doi: 10.1111/j.1467-9574.2012.00523.x

[22] T. C. Headrick and M. D. Pant, A method for simulating nonnormal distributions with specified L-skew, L-kurtosis, and L-correlation, *ISRN Applied Mathematics*, **vol. 2012**, Article ID 980827, 23 pages, (2012). doi: 10.5402/2012/980827

[23] T. C. Headrick and M. D. Pant, A logistic L-moment-based analog for the Tukey g-h, g, h, and h-h system of distributions, *ISRN Probability and Statistics*, **vol. 2012**, Article ID 245986, 23 pages, (2012). doi: 10.5402/2012/245986

[24] T. C. Headrick and M. D. Pant, An L-moment-based analog for the Schmeiser-Deutsch class of distributions, *ISRN Applied Mathematics*, **vol. 2012**, Article ID 475781, 16 pages, (2012). doi:10.5402/2012/475781

[25] J. Karvanen and A. Nuutinen, Characterizing the generalized lambda distributions by L-moments, *Computational Statistics & Data Analysis*, **52**, (2008), 1971-1983.

[26] R. Serfling and P. Xiao, A contribution to multivariate L-moments: L-comoment matrices, *Journal of Multivariate Analysis*, **98**(9), (2007), 1765-1781.

[27] M. C. Jones, On some expressions for variance, covariance, skewness, and L-moments, *Journal of Statistical Planning and Inference*, **126**(1), (2004), 97-106.

[28] Wolfram Mathematica 8.0.4.0 for Microsoft Windows. Wolfram Research, Inc., Champaign, IL, USA, 2011.

[29] S. Wolfram, *The Mathematica Book*, Fifth edition, Wolfram Media, Champaign, IL, USA, 2003.

[30] Microsoft FORTRAN PowerStation Version 4.0. Microsoft Corporation, USA, 1994.

[31] TIBCO Spotfire S+ 8.2.0 for Microsoft Windows. TIBCO Software Inc., Palo Alto, CA, USA, 2010.

[32] G. Marsaglia, Evaluating the Normal Distribution, *Journal of Statistical Software*, **11**(5), (2004), 1-10. http://www.jstatsoft.org/v11/i05

Appendix: Conventional Moments for the Burr Type VII Distributions

The conventional moments associated with Burr Type VII distributions can be obtained by first evaluating the following integral:

$$\mu_r = \int_{-\infty}^{\infty} x^r f(x) dx \tag{A.1}$$

where X is a Burr Type VII random variable with pdf $f(x)$ as given in (3) and where $r = 1, \dots, 4$. In terms of conventional moments, the r-th moment exists only if $k > 0$. Suppose that the first four moments exist, then the conventional moment-based skew and kurtosis can be obtained from Headrick, Pant, and Sheng [14, Equations 12-13]

$$\gamma_3 = (\mu_3 - 3\mu_2\mu_1 + 2\mu_1^3)/(\mu_2 - \mu_1^2)^{3/2} \tag{A.2}$$

$$\gamma_4 = (\mu_4 - 4\mu_3\mu_1 - 3\mu_2^2 + 12\mu_2\mu_1^2 - 6\mu_1^4)/(\mu_2 - \mu_1^2)^2 \tag{A.3}$$

Computing $\mu_{r=1,\dots4}$ from (A.1) and substituting in (A.2)—(A.3) and simplifying yields the following system of equations for characterizing the Burr Type VII distribution through the method of conventional moments:

$$\mu = \frac{1}{2}(k\text{H1}[\{1,1,1+k\},\{2,2\},-1] - \Gamma[k]\text{H2}[k,k,1+k,-1]) \tag{A.4}$$

$$\sigma = (2k)^{-1}\{2(\text{H1}[\{k,k,k\},\{1+k,1+k\},-1]$$
$$+ k^3\text{H1}[\{1,1,1,1$$
$$+ k\},\{2,2,2\},-1])-(k^2\text{H1}[\{1,1,1+k\},\{2,2\},-1]$$
$$- \text{H2}[k,k,1+k,-1])^2\}^{1/2} \tag{A.5}$$

$$\gamma_3 = \{2(8^{-k}(-1-k^2\Gamma[k]\text{H2}[1,1,2+k,-1] \tag{A.6}$$

$$+ 2^k k^2 \text{H1}[\{1,1,1+k\},\{2,2\},-1])^3 +$$

$$3 \times 2^{-k}(1+k^2\Gamma[k]\text{H2}[1,1,2+k,-1]-2^k k^2\text{H1}[\{1,1,1+k\},\{2,2\},-1])$$

$$\times$$

$$(\text{H1}[\{k,k,k\},\{1+k,1+k\},-1]+k^3\text{H1}[\{1,1,1,1+k\},\{2,2,2\},-1])-3\times$$

$$\text{H1}[\{k,k,k,k\},\{1+k,1+k,1+k\},-1]$$

$$+ 3k^4\text{H1}[\{1,1,1,1,1+k\},\{2,2,2,2\},-1])\}/$$

$$\{-4^{-k}(1+k^2\Gamma[k]\text{H2}[1,1,2+k,-1]-2^k k^2\text{H1}[\{1,1,1+k\},\{2,2\},-1])^2$$

$$+$$

$$2(\text{H1}[\{k,k,k\},\{1+k,1+k\},-1]+k^3\text{H1}[\{1,1,1,1+k\},\{2,2,2\},-1]\}^{3/2}$$

$$\gamma_4 = \{2k^4(-3\times 2^{-4k}k^4(1/k^2+\Gamma[k]\text{H2}[1,1,2+k,-1] \tag{A.7}$$

$$- 2^k\text{H1}[\{1,1,1+k\},\{2,2\},-1])^4$$

$$+ 3\times 4^{1-k}(1/k^2$$

$$+ \Gamma[k]\text{H2}[1,1,2+k,-1]-2^k\text{H1}[\{1,1,1+k\},\{2,2\},-1])^2\times$$

$$(\text{H1}[\{k,k,k\},\{1+k,1+k\},-1]+k^3\text{H1}[\{1,1,1,1+k\},\{2,2,2\},-1])$$

$$- 6/k^4\times$$

$$(\text{H1}[\{k,k,k\},\{1+k,1+k\},-1]+k^3\text{H1}[\{1,1,1,1+k\},\{2,2,2\},-1])^2$$

$$- 3/k^4\times$$

$$2^{2-k}(-1-k^2\Gamma[k]\text{H2}[1,1,2+k,-1]+2^k k^2\text{H1}[\{1,1,1+k\},\{2,2\},-1])\times$$

$$(-\text{H1}[\{k,k,k,k\},\{1+k,1+k,1+k\},-1]$$

$$+ k^4\text{H1}[\{1,1,1,1,1+k\},\{2,2,2,2\},-1])$$

$$+ 12/k^4 (\text{H1}[\{k,k,k,k,k\},\{1+k,1+k,1+k,1+k\},-1]+k^5\times$$

$$\text{H1}[\{1,1,1,1,1,1+k\},\{2,2,2,2,2\},-1]))\}/\{4^{-k}(1+k^2\Gamma[k]\text{H2}[1,1,2$$

$$+ k,-1]-$$

$$2^k k^2\text{H1}[\{1,1,1+k\},\{2,2\},-1])^2-2(\text{H1}[\{k,k,k\},\{1+k,1+k\},-1]+$$

$$k^3\text{H1}[\{1,1,1,1+k\},\{2,2,2\},-1])\}^2$$

where the usual definitions of mean (μ) and standard deviation (σ) were used to obtain (A.4) and (A.5) and $\Gamma[.] = \text{Gamma}[.]$, $\text{H1}[.] = \text{HypergeometricPFQ}[.]$, and $\text{H2}[.] = \text{Hypergeometric2F1}[.]$ are inbuilt Mathematica [28] functions,

respectively.

Thus, for given value of kurtosis (γ_4), the shape parameter (k) can be determined by solving (A.7), using Mathematica [28] function FindRoot. The solved value of k can then be substituted into (A.4)—(A.6) for computing the values of mean (μ), standard deviation (σ), and skew (γ_3), respectively, associated with the Burr Type VII distribution.